

1 **Running Head: Wettability and water uptake of holm oak leaf surfaces**

2

3 **Corresponding authors:**

4 **Victoria Fernández**

5 Forest Genetics and Ecophysiology Research Group

6 School of Forest Engineering

7 Technical University of Madrid

8 Ciudad Universitaria s/n

9 28040 Madrid

10 Spain

11 Phone number: +34 91 3367113

12 FAX: +34 91 3365556

13 v.fernandez@upm.es

14

15 **Eustaquio Gil-Pelegrín**

16 Unidad de Recursos Forestales

17 Centro de Investigación y Tecnología Agroalimentaria

18 Gobierno de Aragón

19 50059 Zaragoza

20 Spain

21 Phone number: +34 976 716394

22 FAX: +34 976 716335

23 egilp@aragon.es

24

25

26 **Research Area: Ecophysiology and Sustainability**

27

28

29 **Wettability, polarity and water absorption of *Quercus ilex* leaves: effect of leaf side**
30 **and age**

31

32 Victoria Fernández^{1,†,*}, Domingo Sancho-Knapik^{2,†}, Paula Guzmán¹, José Javier
33 Peguero-Pina², Luis Gil¹, George Karabourniotis³, Mohamed Khayet⁴, Costas Fasseas⁵,
34 , José Alejandro Heredia-Guerrero⁶, Antonio Heredia⁷ and Eustaquio Gil-Pelegrín^{2,*}

35

36 *Corresponding authors

37 †Both authors contributed equally to this work

38

39 ¹Forest Genetics and Ecophysiology Research Group, School of Forest Engineering,
40 Technical University of Madrid, Ciudad Universitaria s/n, 28040 Madrid, Spain

41 ²Unidad de Recursos Forestales, Centro de Investigación y Tecnología Agroalimentaria,
42 Gobierno de Aragón, 50059 Zaragoza, Spain

43 ³Laboratory of Plant Physiology, Department of Crop Science, Agricultural University
44 of Athens, Iera Odos 75, 118 55, Botanikos, Athens, Greece

45 ⁴Department of Applied Physics I, Faculty of Physics, Universidad Complutense, Avda.
46 Complutense s/n, 28040 Madrid, Spain

47 ⁵Laboratory of Electron Microscopy, Department of Crop Science, Agricultural
48 University of Athens, Iera Odos 75, 118 55, Botanikos, Athens, Greece

49 ⁶Nanophysics, Istituto Italiano di Tecnologia, Via Morego 30, 16163, Genoa, Italy

50 ⁷Molecular Biology and Biochemistry Department, Instituto de Hortofruticultura
51 Subtropical Mediterránea (IHSM) La Mayora. CSIC-UMA, 29071 Málaga, Spain

52

53

54

55

56

57 **Summary**

58

59 The highly pubescent abaxial side of *Q. ilex* leaves is unwettable and water-repellent.
60 The adaxial side is however wettable and can take up water, which may be an
61 adaptation to growing under Mediterranean conditions

62

63 Footnotes

64

65 Victoria Fernández is supported by a “Ramón y Cajal” contract (MINECO, Spain) co-
66 financed by the European Social Fund. Paula Guzmán is supported by a pre-doctoral
67 grant from the Technical University of Madrid. Work of José Javier Peguero-Pina was
68 supported by a ‘Juan de la Cierva’-MICIIN post-doctoral contract. This study was
69 supported by the Spanish Ministry of Economy and Competitiveness (MINECO, Spain;
70 Projects AGL2010-21153-C02-02 and AGL2012-35580).

71

72

73 Corresponding authors: Eustaquio Gil-Pelegrín, email: egilp@aragon.es; Victoria
74 Fernández: v.fernandez@upm.es

75

76

77

78 **ABSTRACT**

79 Plant trichomes play important protective functions and may have a major influence on
80 leaf surface wettability. With the aim of gaining insight into trichome structure,
81 composition and function in relation to water-plant surface interactions, we analyzed the
82 adaxial and abaxial leaf surface of *Quercus ilex* L. (holm oak) as model. By measuring
83 the leaf water potential 24 h after the deposition of water drops on to abaxial and adaxial
84 surfaces, evidence for water penetration through the upper leaf side was gained in young
85 and mature leaves. The structure and chemical composition of the abaxial (always
86 present) and adaxial (occurring only in young leaves) trichomes were analyzed by
87 various microscopic and analytical procedures. The adaxial surfaces were wettable and
88 had a high degree of water drop adhesion in contrast to the highly unwettable and water
89 repellent abaxial holm oak leaf sides. The surface free energy, polarity and solubility
90 parameter decreased with leaf age, with generally higher values determined for the
91 abaxial sides. All holm oak leaf trichomes were covered with a cuticle. The abaxial
92 trichomes were composed of 8% soluble waxes, 49% cutin, and 43% polysaccharides.
93 For the adaxial side, it is concluded that trichomes and the scars after trichome shedding
94 contribute to water uptake, while the abaxial leaf side is highly hydrophobic due to its
95 high degree of pubescence and different trichome structure, composition and density.
96 Results are interpreted in terms of water-plant surface interactions, plant surface
97 physical-chemistry, and plant ecophysiology.

98

99 **INTRODUCTION**

100 Plant surfaces have an important protecting function against multiple biotic and
101 abiotic stress factors (Riederer, 2006). They may for example limit the attack of insects
102 (Eigenbrode and Jetter, 2002), or pathogenic fungi (Gniwotta et al., 2005; Łaźniewska
103 et al., 2012), avoid damage caused by high intensities of UV and visible radiation
104 (Reicosky and Hanover, 1978; Karabourniotis and Bormann, 1999), help to regulate
105 leaf temperature (Ehleringer and Björkman, 1978; Ripley et al., 1999), and chiefly
106 prevent plant organs from dehydration (Riederer and Schreiber, 2001).

107 The epidermis of plants has been found to have major degree of physical and
108 chemical variability, and may often contain specialised cells such as trichomes or
109 stomata (Roth-Nebelsick et al., 2009; Javelle et al., 2011). Most aerial organs are
110 covered with an extra-cellular, generally lipid-rich layer named cuticle, which is
111 typically composed of waxes embedded into (intra-cuticular) or deposited on to (epi-
112 cuticular waxes) a biopolymer matrix of cutin (forming a network of cross-esterified,
113 hydroxy C₁₆ and/or C₁₈ fatty-acids) and/or cutan, with variable amounts of
114 polysaccharides and phenolics (Domínguez et al., 2011; Yeats and Rose, 2013).
115 Different nano- and/or micro-scale levels of plant surface sculpturing have been
116 observed by scanning electron microscopy (SEM), generally in relation to the
117 topography of epicuticular waxes, cuticular folds and epidermal cells (Koch and
118 Barthlott, 2009). Such surface features together with their chemical composition
119 (Khayet and Fernández, 2012) may lead to a high degree of roughness and
120 hydrophobicity (Koch and Barthlott, 2009; Konrad et al., 2012). The interactions of
121 plant surfaces with water have been addressed in some investigations (Brewer et al.,
122 1991; Brewer and Schmidt, 1997; Pandey and Nagar, 2003; Hanba et al., 2004; Dietz et
123 al., 2007; Holder, 2007a, b; Fernández et al., 2011, 2014; Roth-Nebelsick et al., 2012;
124 Wen et al., 2012; Urrego-Pereira et al., 2013), and is a topic of growing interest for
125 plant ecophysiology (Helliker and Griffiths, 2007; Aryal and Neuner, 2010; Limm and
126 Dawson, 2010; Kim and Lee, 2011; Berry and Smith, 2012; Rosado and Holder, 2013;
127 Berry et al., 2013; Helliker, 2014). On the other hand, the mechanisms of foliar uptake
128 of water and solutes by plant surfaces are still not fully understood (Fernández and
129 Eichert, 2009; Burkhardt and Hünsche, 2013), but they may play an important
130 ecophysiological role (Limm et al., 2009; Johnstone and Dawson, 2010; Adamec, 2013;
131 Berry et al., 2014).

132 The importance of trichomes and pubescent layers on water drop-plant surface
133 interactions and on the subsequent potential water uptake into the organs has been
134 analysed in some investigations (Fahn, 1986; Brewer et al., 1991; Grammatikopoulos
135 and Manetas, 1994; Brewer and Smith, 1997; Pierce et al., 2001; Kenzo et al., 2008;
136 Fernández et al., 2011, 2014; Burrows et al., 2013). Trichomes are unicellular or multi-
137 cellular, glandular or non-glandular appendages, which originate from epidermal cells
138 only, and develop outwards on the surface of plant organs (Werker, 2000). Non-
139 glandular trichomes are categorised according to their morphology and exhibit a major
140 variability in size, morphology, and function. On the other hand, glandular trichomes
141 are classified by the secretory materials they excrete, accumulate or absorb (Johnson,
142 1975; Werker, 2000; Wagner et al., 2004). Trichomes can be often found in
143 xeromorphic leaves and in young organs (Fahn, 1986; Karabourniotis et al., 1995). The
144 occurrence of protecting leaf trichomes has been also reported for Mediterranean
145 species such as *Quercus ilex* L. (Karabourniotis et al., 1995, 1998; Morales et al., 2002;
146 Karioti et al., 2011; Camarero et al., 2012). There is limited information about the
147 nature of the surface of trichomes, but they are also covered with a cuticle similarly to
148 other epidermal cell types (Fernández et al., 2011, 2014).

149 In this study and using *Q. ilex* as model, we assessed for the first time the leaf
150 surface-water relations of the abaxial (always pubescent) versus the adaxial (only
151 pubescent in developing leaves and for a few months) surface, including their capacity
152 to absorb surface-deposited water drops. Based on membrane science methodologies
153 (Fernández et al., 2011; Khayet and Fernández 2012) and following a new integrative
154 approach, the chemical, physical and anatomical properties of holm oak leaf surfaces
155 and trichomes were analyzed, with the aim of addressing the following questions: (i) are
156 young and mature adaxial and abaxial leaf surfaces capable of absorbing water
157 deposited as drops on to the surfaces?, (ii) are young and mature abaxial and adaxial
158 leaf surfaces similar in relation to their wettability, hydrophobicity, polarity, work-of-
159 adhesion for water, solubility parameter and surface free energy?, and (iii) what is the
160 physical and chemical nature of the adaxial versus the abaxial trichomes, chiefly in
161 relation to young leaves?

162

163 **RESULTS**

164 **Leaf surface water absorption**

165 The water absorption results for both young and mature holm oak shoots are shown
166 in Figure 1. The initial shoot water potential (Ψ_o) measured for young shoots were -2.47
167 ± 0.10 MPa. Twenty-four h after wetting the adaxial side of the leaves, the final water
168 potential (Ψ_f) became -1.51 ± 0.15 MPa. In contrast, after wetting the abaxial side, Ψ_f
169 reached -3.00 ± 0.09 MPa. As expected, the untreated (non-wetted) shoots, reached a
170 lower Ψ_f of -3.19 ± 0.07 MPa (Fig. 1A). All Ψ_f values were statistically different from
171 Ψ_o ($\alpha = 0.05$). A similar trend was found for mature shoots (Fig. 1B). In addition, the
172 relative water content (RWC) varied according to the water potential variations. When
173 the adaxial holm oak leaf side was wetted, RWC increased from 88.79 ± 0.54 to $93.45 \pm$
174 0.67% . When drops were applied on to the abaxial side, RWC decreased from $87.52 \pm$
175 0.63 to $84.22 \pm 0.65\%$. Finally, the RWC of untreated leaves (non-wetted) decreased
176 from 88.05 ± 0.99 to $82.48 \pm 0.89\%$ (Fig. 1C). Similar variations were recorded for
177 mature leaves (Fig. 1D).

178 The adaxial and abaxial surface cuticular conductances of young holm-oak leaves
179 were 3.8 ± 0.2 and $3.4 \pm 0.1 \text{ m s}^{-1} 10^{-5}$, respectively. The cuticular conductance values
180 measured for mature leaves were 3.1 ± 0.2 (adaxial) and 3.3 ± 0.3 (abaxial) $\text{m s}^{-1} 10^{-5}$.
181 Regardless of leaf age, no significant cuticular conductance differences were found
182 between upper and lower leaf sides. Statistically significant conductance differences
183 were however recorded for the adaxial cuticle of young versus mature leaves ($P < 0.05$).

184 **Holm oak leaf surface structure**

185 Fresh, young and mature holm oak leaves were examined by SEM. The young leaves
186 were covered with trichomes, the adaxial surfaces being much less pubescent than the
187 abaxial surfaces, where dense, imbricated trichome layers were found (Fig. 2, A and B).
188 An abaxial dense indumentum was also present in mature leaves, but their upper
189 surfaces had almost no trichomes (Fig. 2, C and D).

190 Concerning the adaxial leaf epidermis, a rather smooth epicuticular wax layer could
191 be observed in mature leaves, which was only partially visible as patches in the young
192 leaves (Fig. 2, A and C). The adaxial side of young leaves had a trichome density of
193 approximately 87 per mm^2 leaf surface. The cuticle surface covered with trichomes was

194 estimated to be about 43% (Fig. 2A). Some protruding trichome-scars were especially
195 visible in the mature leaf adaxial surface (Fig. 2C).

196 Trichomes were observed to be non-glandular, multicellular, stellate, with the arms
197 fusing into a short, erect stipe and then diverging horizontally (Hardin, 1976). Most of
198 the adaxial trichomes of the young leaves had eight arms, while single long hairs, and
199 from four to seven-arm-trichomes were also eventually found. Their length and
200 diameter were measured on eight-arm-trichomes from the fusing point and at 10 μm
201 above, respectively. The length of the arms was approximately $115 \pm 24 \mu\text{m}$, and the
202 diameter was $6.2 \pm 0.6 \mu\text{m}$. The overlapping of trichome arms and the existence of
203 various trichome layers on the lower leaf sides prevented the accurate estimation of the
204 number of arms, arm length and diameter.

205 When analyzing the epidermal structure of holm oak leaves we noticed that the base
206 of abaxial and adaxial trichomes was cutinized, since it was stained with Sudan IV (Fig.
207 3A). The structure of the base of adaxial versus abaxial trichomes is different (Fig. 3, B
208 to E). Abaxial trichomes are anchored deeper into the epidermis by a group of cells
209 (Fig. 3, C and E), while those present in the upper side of young leaves are bound to the
210 underlying tissue in a more superficial manner, the union largely formed by cuticle and
211 cell wall material appearing more susceptible to shedding (Fig. 3, B and D). The scars
212 remaining in the upper leaf sides after trichome abscission seemed to have a
213 heterogeneous topography in both young (Fig. 3F) and mature leaves (Fig. 3G).
214 Trichomes and trichome scars were often seen directly or in the vicinity of bundle
215 sheath extensions (Fig. 3, A and G).

216 **Chemical composition of trichomes**

217 The proportion of chemical constituents of isolated holm oak trichomes was assessed
218 by the weight loss after successive chemical treatments, coupled with Fourier transform
219 infrared spectroscopy (FTIR) measurements. Isolated trichome SEM observations,
220 however, led us to discard the data concerning the adaxial side, since epidermal pieces
221 of considerable size were removed together with the trichomes due to their scarcity.
222 Hence, we are only showing the chemical composition of trichomes isolated from the
223 lower leaf side to avoid misinterpretations.

224 The fractions corresponding to depolymerized material (chiefly cutin) represented
225 the greatest percentage of the trichomes (49.0%). After cutin depolymerization a residue

226 (mainly of polysaccharides) of 42.9% was determined. A proportion of soluble waxes of
227 7.9% of the trichome mass was recorded after chloroform extraction.

228 The FTIR spectra of isolated intact and chemically treated abaxial holm oak
229 trichomes are shown in Figure 4. Cuticular material assignment was based on previous
230 data (Ramírez et al., 1992; Villena et al., 2000). For intact hairs, bands associated with
231 different chemical functional groups, and consequently to cuticle components, were
232 identified (Fig. 4A): long-chain aliphatic waxes and cutin (intense and thin asymmetric
233 and symmetric CH₂ stretching absorptions at 2919 and 2849 cm⁻¹ and the CH₂ bending
234 one at 1463 cm⁻¹), the polyester cutin (C-O stretching vibration in ester environments
235 band at 1729 cm⁻¹ and the asymmetrical and symmetrical C-O-C stretching absorptions
236 at 1166 and 1107 cm⁻¹, respectively), polysaccharides (mainly for the band associated
237 with the glycosidic bond at 1054 cm⁻¹), and some unsaturated/aromatic compounds
238 (stretching of C=C double bonds, aromatic rings, and aromatic rings conjugated with
239 double bonds at 1653, 1610 and 1515 cm⁻¹, respectively). The broad and very strong
240 band at 3350 cm⁻¹, assigned to the O-H stretching vibration, could be related to tissue
241 hydration. When waxes were extracted in chloroform, a remarkable reduction of the
242 aliphatic bands was observed (CH₂ stretching absorptions decreased and broadened;
243 Fig. 4B). Finally, the saponification step led to the depolymerization of cutin and hence
244 decreasing its characteristic absorption peaks. The remaining material can be considered
245 a polysaccharide fraction with a small contribution of unsaturated/aromatic compounds
246 (Fig. 4C).

247 When examining the isolated trichomes of young holm oak leaves by SEM, a
248 generally smoother surface with some shallow cracks was noticed after wax removal as
249 compared to the intact trichomes (Fig. 5, A to D). This phenomenon could be observed
250 more clearly in the abaxial trichomes, since they initially had a rougher epicuticular wax
251 layer as compared to adaxial ones (Fig. 5, B and D). After cutin depolymerization,
252 trichomes appeared to be flatter, with twisted arms, and showing the cell wall structure
253 (Fig. 5, E and F). Adaxial, intact (isolated and attached to the leaf surface) and
254 chloroform-extracted trichomes seemed to be covered with only a partially-developed
255 cuticle (Figs. 5, A and C and 6A).

256 The effect of immersing holm oak leaves in cellulase and pectinase solutions for 4 or
257 7 days is shown in Figure 6. The adaxial trichomes of young leaves were hydrolyzed
258 when immersed in 2% cellulase (Fig. 6C). The process of trichome degradation seemed
259 to take place from the fusing point of each arm at the side which is exposed to the

260 environment (Fig. 6B). After seven days of cellulase hydrolysis, almost only the cuticle
261 covering the base of the trichomes remained attached to the epidermis underneath (Fig.
262 6C), which finally led to trichome shedding. The opening of the cuticle fusing line
263 (observed as a central furrow in the arms) located near the base in some arms of intact
264 trichomes (Fig. 6A) may somehow facilitate cellulase accessibility and cell wall
265 degradation. These cuticular fractures in the adaxial trichomes were more common in
266 the fusing point and towards the tip of the arms (see Fig. 6A as an example). Leaf
267 immersion in cellulase did not alter the structure of abaxial leaf trichomes which were
268 similar to those present in intact holm oak surfaces (Fig. 6D). Leaf pectinase digestion
269 did not affect the structure of either the adaxial or the abaxial trichomes (data not
270 shown).

271 **Contact angle measurements**

272 The mean θ values measured after depositing drops of three liquids with different
273 polar and apolar surface tension components on to the adaxial and abaxial surfaces of
274 young and mature holm oak leaves are summarized in Table I. The presence of
275 trichomes in young leaf adaxial surfaces led to initially high θ values for water and
276 especially glycerol, which sharply decreased over time before reaching a steady value
277 when the drop became static. This phenomenon was however not observed for the fully
278 apolar diiodomethane drops which remained static when deposited on to the adaxial
279 young leaf surfaces. This indicates that water and glycerol drops (having a significant
280 polar (acid-base) surface tension component) interacted with the trichomes present in
281 the adaxial surface of young leaves which led to a sharp θ decrease shortly after drop
282 deposition (Fig. 2A; Table I). On the contrary, the glabrous upper leaf surface of mature
283 leaves and the highly pubescent abaxial young and mature leaf surfaces enabled the
284 measurement of static contact angles immediately after drop deposition which implies a
285 lower degree of chemical interactions between such liquids and the plant surfaces
286 analyzed (Fig. 2, B to D).

287 With regard to leaf age, higher water and glycerol θ values were measured on the
288 upper side of mature versus young leaves, but similar results were recorded for all
289 abaxial leaf surfaces. In contrast, diiodomethane θ measurements were similar for the
290 adaxial surface of young and mature leaves and slightly higher for the abaxial side of
291 young leaves.

292 The total surface free energy (γ) of the holm oak leaf surfaces evaluated was
293 determined from contact angle measurements (Fernández et al., 2011, 2014) using the
294 so-called Lifshitz-van der Waals, van Oss, Good, and Chaudhury method (van Oss et
295 al., 1987, 1988). The γ of young leaf adaxial surfaces was higher than that of mature
296 surfaces (Table II). In contrast, the abaxial surface of mature leaves had a higher γ value
297 as compared to the upper side. On the other hand, the total γ results of young and mature
298 adaxial leaf surfaces were higher than the values determined for the corresponding
299 abaxial surfaces. The γ values of the upper surfaces can be mainly ascribed to their
300 relatively higher dispersive component (γ^{LW}). For the adaxial surface, the non-dispersive
301 component (γ^{AB}) was higher for young leaves and decreased with maturity (Table II).

302 The highest degree of surface polarity was generally determined for the abaxial leaf
303 side. For the upper side, the surface polarity values of young leaves were however
304 higher than those determined for mature leaves (Table II).

305 The work-of-adhesion (W_a ; Kwok and Neumann, 1999) for the three liquids and the
306 solubility parameter (δ) were calculated as described by Fernández et al. (2011, 2014)
307 and Khayet and Fernández (2012) (Table III). The adaxial surface of young and mature
308 holm oak leaves exhibited a higher adhesion for water drops, followed by glycerol and
309 diiodomethane, compared to the water drop repellence of the lower leaf side. Of the
310 three liquids, the highest W_a values were recorded for water drops deposited on to the
311 upper leaf side. Regardless of leaf age, the abaxial surfaces were found to have similar
312 W_a values for water and diiodomethane, which were higher than those for glycerol. The
313 solubility parameter (δ) values of the adaxial surface of young and mature leaves were
314 considerably higher than those of the lower leaf side. Regarding the effect of leaf age,
315 younger leaves had higher δ values as compared to mature leaves.

316 **DISCUSSION**

317 In this study, we analyzed the physico-chemical properties of the adaxial and abaxial
318 surface of holm oak (*Q. ilex L.*) leaves as model for a typically Mediterranean species,
319 and also in relation to leaf maturity. We selected this species since it constitutes an
320 interesting system for assessing the nature and functionality of adaxial and abaxial leaf
321 surfaces, and also for evaluating leaf water absorption and solid-liquid interactions. As a
322 preliminary trial, we assessed the water absorption capacity of holm oak leaves by
323 measuring the leaf water potential 24 h after depositing water drops either on to the
324 adaxial or abaxial leaf side. After gaining evidence for leaf hydration via the upper leaf

325 side (independently of leaf age), we analyzed in detail the physico-chemical and
326 structural properties of abaxial and adaxial holm oak leaf surfaces, focussing on
327 trichomes. The structure and morphology of the adaxial and abaxial trichomes were
328 similar to those described in previous holm oak leaf studies (e.g., Karabourniotis et al.,
329 1998; Karioti et al., 2011; Camarero et al., 2012).

330 **Trichome chemical composition and structure**

331 The presence of trichomes in developing organs has been reported in previous
332 studies (e.g., Karabourniotis et al., 1995). The adaxial and abaxial holm oak leaf side
333 performed differently in terms of wettability (Table I), as previously found for other
334 plant species (e.g., Brewer and Smith, 1997; Fernández et al., 2014). We showed that
335 the hydrophobic character of the abaxial leaf side is clearly associated with the
336 roughness provided by the high density, chemical composition and structure of
337 trichomes. According to the classification suggested by Brewer et al. (1991) and Brewer
338 and Smith (1997) the abaxial oak leaf trichomes may belong to the “lifting strategy”
339 group, while further trials will required for characterizing the performance of liquid
340 water with the adaxial oak leaf side at a macroscopic level.

341 Leaf surface hydrophobicity has been often interpreted as either an adaptive trait to
342 dry climates (Holder, 2007a) or to wet environments (Holder, 2007b). The occurrence
343 of trichome layers on the abaxial leaf surface may be considered as a xeromorphic
344 character which provides adaptive advantages mainly under biotic and abiotic stress
345 conditions (Karabourniotis et al., 1992; Karabourniotis and Bormman, 1999;
346 Liakopoulos et al., 2006). In spite of this, the relationship between leaf surface
347 hydrophobicity and the ecological conditions where a plant species is native to remains
348 controversial.

349 By measuring the contact angles of three liquids with different polarity, we gained
350 evidence for the wettable character of holm oak adaxial leaf surfaces. The increased
351 wettability and work-of-adhesion for water of the adaxial young leaf surfaces is
352 associated with the occurrence of hydrophilic trichomes, which interacted with polar
353 liquids (i.e., water and glycerol) immediately after drop deposition. The degradation of
354 adaxial trichomes after leaf immersion in cellulase showed that they were permeable to
355 water in contrast to the abaxial ones which were not altered by the enzymatic treatment.
356 The cuticular irregularities observed in the surface and base of the adaxial trichomes are

357 likely to be the main uptake pathway for the cellulase solution, which finally led to
358 trichome degradation.

359 The gradual extraction of cuticular components of the abaxial leaf surface trichomes
360 coupled to SEM observations, facilitated the quantification of cuticular constituents
361 which amounted to 8% soluble waxes, 49% depolymerized material (likely cutin) and
362 43% residue (chiefly polysaccharides). The adaxial holm oak leaf trichomes were
363 largely found to have a higher proportion of cutin and a lower content of
364 polysaccharides as compared to the peach fruit trichomes analyzed by Fernández et al.
365 (2011; having 15% waxes, 19% cutin and 66% polysaccharides). Scanning and
366 transmission electron microscopy observations also in relation to the chemical removal
367 of cuticular components showed that both the adaxial and abaxial trichomes are covered
368 with a cuticle, which seemed to be homogeneously distributed along the surface of the
369 more long-lasting, abaxial trichomes but appeared to develop heterogeneously over the
370 cell wall of the adaxial trichomes of young holm oak leaves. Apart from being
371 hydrophilic, such trichomes fractured more easily. Moreover, trichome shedding left a
372 scar on the adaxial leaf surface, and the base of the abscised trichomes may represent a
373 site for water entry since the cuticle in this area was observed to be thinner and more
374 heterogeneous (Fig. 3, F and G). In addition, adaxial trichomes were often located in the
375 vicinity of bundle sheath extensions (Fig. 3, F and G). Bundle sheath extensions may
376 facilitate the transport of water in such heterobaric leaves (Wylie, 1943), and may be
377 related to water economy (Nikolopoulos et al., 2002).

378 **Leaf surface wettability, polarity, solubility parameter and work-of-adhesion**

379 Measurement of water contact angles provides information about the wettability and
380 retention of water drops by different leaf surfaces, and may serve as tool to classify
381 species growing in contrasting environmental conditions (e.g., Brewer et al., 1991;
382 Brewer and Nuñez, 2007; Holder, 2007a, b). Additional determinations of contact
383 angles of liquids with different polarity (Fernández et al., 2011; Khayet and Fernández,
384 2012), facilitate the quantitative characterisation of plant surfaces and their solid-liquid
385 interactions, in relation to the combined effect of surface chemistry and roughness.

386 The most abundant epicuticular waxes found on *Q. ilex* young leaves are *n*-alkyl
387 esters, representing up to 56% of the total chloroform soluble waxes, followed by *n*-
388 primary alcohols (Martins et al., 1999). While an increased surface roughness due to
389 pubescence (Fernández et al., 2011) seems again to have a major effect on leaf surface

390 wettability, the contribution of surface chemistry should also be considered, and is the
391 major factor affecting water-solid interactions in the adaxial surface of mature leaves
392 (rather flat and glabrous). The predominant role of surface chemistry in relation to the
393 adaxial, mature leaf side was supported by the solubility parameter value obtained
394 experimentally (approximately $16 \text{ MJ}^{1/2} \text{ m}^{-3/2}$), which is within the range calculated by
395 Khayet and Fernández (2012) for model epicuticular wax molecular structures (between
396 16 to $17 \text{ MJ}^{1/2} \text{ m}^{-3/2}$). In contrast, the dense indumentum of the lower leaf sides led to
397 extremely low solubility parameter values, which were even below those determined for
398 the almost super-hydrophobic juvenile *Eucalyptus globulus* leaf surface (Khayet and
399 Fernández, 2012). This may be due to the high level of surface roughness and to the
400 occurrence of air pockets within the trichome layers covering the abaxial leaf side
401 (Fernández et al., 2011), which may be even denser when leaves are young.

402 Irrespective of leaf age, the upper leaf side had a higher surface free energy than the
403 lower one, while polarity followed an inverse trend. The work-of-adhesion for water
404 provides a quantification of the degree of water drop adhesion or repulsion to a certain
405 plant surface (Fernández et al., 2014). The work-of-adhesion for water was extremely
406 high for the adaxial holm oak leaf surface as compared to the values previously obtained
407 for other pubescent or glabrous plant materials (Khayet and Fernández, 2012; Fernández
408 et al., 2014). The presence of trichomes in the adaxial side of the young holm oak leaves
409 additionally increased the adhesion of water drops to such surfaces. However, the lower
410 leaf sides had a degree of water drop repulsion similar to the one of the peach fruit
411 (Fernández et al., 2011), but their work-of-adhesion for water was above the values
412 estimated for the even more water-repellent and unwettable, hairy, adaxial wheat leaf
413 surface (Fernández et al., 2014).

414 **Leaf water uptake and ecophysiological implications**

415 The ability to capture water via the leaf has been indirectly reported in species
416 occurring in deserts (Martin and von Willert, 2000), tropical climates (Yates and
417 Hutley, 1995), cloud-immersed mountain habitats (Berry and Smith, 2012; Berry et al.,
418 2013, 2014) and in coastal mountain regions where fog is a significant climatic
419 contributor (Burgess and Dawson, 2004). However, this is the first time when foliar
420 water uptake has been analysed in strict physico-chemical terms, while recording
421 significant water potential changes in response to leaf hydration.

422 Regardless of leaf age, we observed a markedly different performance of the adaxial
423 (wetttable and retaining water drops) versus the abaxial (unwetttable and water-repellent)
424 holm oak leaf surfaces when in contact with water drops. We have demonstrated that
425 the major wettability of the adaxial side of holm oak leaves allows for leaf rehydration
426 both in terms of RWC and leaf water potential (Fig. 1). Drop adherence to the plant
427 surface is a pre-requisite for foliar uptake to occur (Fernández and Brown, 2013;
428 Fernández et al., 2014). Thereby, in the case of holm oak leaves, foliar absorption of
429 pure water (i.e., in the absence of surfactants) may only take place through the upper
430 leaf side to which water drops strongly adhere (having a high work-of-adhesion for
431 water; Table III). In contrast, the repulsion of water drops by the abaxial leaf side will
432 impede the penetration of liquid water. The hydrophobic nature of the abaxial leaf
433 trichomes will ensure the occurrence of an air layer above stomatal pores, and hence
434 help to preserve an adequate gas exchange rate even under wet conditions.

435 The permeability of plant surfaces to water and solutes has been a matter of scientific
436 interest since the last century, but the mechanisms involved are still not fully
437 characterised (Fernández and Eichert, 2009). Water deposited on to a leaf surface may
438 penetrate via stomata, the cuticle, cuticular cracks and irregularities, or through
439 specialised epidermal cells such as trichomes (Fernández and Brown, 2013). In the case
440 of holm oak adaxial leaf surfaces, trichomes and the remaining scars after trichome
441 shedding may play a key role in water absorption. The high surface tension, polarity and
442 H-bonding capacity of water theoretically pose restrictions for the penetration of this
443 liquid through the cuticle (Guzmán et al., 2014 a,b) and also via stomata (Schönherr and
444 Bukovac, 1972; Burkhardt et al., 2012). The actual contribution of leaf trichomes to the
445 absorption of water and solutes remains unclear (Fernández et al., 2014). While some
446 studies suggest that trichomes may actively participate in the uptake of foliar-applied
447 nutrient solutions (e.g., Benzing et al., 1976; Schlegel and Schönherr, 2002), and water
448 in Bromeliads (e.g., Pierce et al., 2001; Reyes-García et al., 2011), the contribution of
449 *Phlomis fruticosa* leaf trichomes to the absorption of water could not be clarified
450 (Grammatikopoulos and Manetas, 1994). A traditional problem when investigating on
451 the mechanisms of foliar penetration is the occurrence of technical constraints
452 associated with optical and fluorescence microscopy and attempting to observe the
453 uptake of specific dyes and solutes by leaf surface micro- and nano-structures
454 (Fernández and Eichert, 2009). Fahn (1986) and more recently Burrows et al. (2013)
455 reported that leaf trichomes having a cutinised base would fail to take up the surface-

456 applied dye solutions and to transport them into the leaf interior. While the base of the
457 adaxial and abaxial holm oak leaf trichomes that we analysed was cutinised, when
458 applying water drops on to the adaxial surface of young *Q. ilex* leaves we gained
459 evidence for hydration as derived from the resulting leaf water potential increase . Our
460 results suggest that there may be a major degree of variability among trichome
461 structures and functions that may sometimes impede or facilitate the uptake of water.

462 Foliar water uptake due to natural phenomena such as fog or dew may be an
463 important mechanism of hydration in some areas of the world subjected to temporary
464 drought (e.g., Burgess and Dawson, 2004; Oliveira et al., 2005; Breshears et al., 2008;
465 Limm et al., 2009; Simonin et al., 2009; Limm and Dawson, 2010; Berry et al., 2013,
466 2014; Gotsch et al., 2014).

467 Holm oak is a species native to Mediterranean-type climates where summer drought
468 is imposed by a combination of high temperatures and low precipitation. In spite of the
469 lower precipitation level during this season, summer rainfall constitutes 24% of the
470 whole year precipitation (referring to the Iberian Peninsula; www.aemet.es). In this
471 season, short-term storms are the most common precipitation form, being up to 100% of
472 the fallen rain during July and August (Mosmann et al., 2004). While most of the water
473 falling after high precipitation summer storms is not available for plant roots due to
474 storm water run-off, low precipitation storms (below 1 mm) are considered negligible in
475 terms of soil water balance (Allen et al., 2000), the latter accounting for 54% of the total
476 summer rainfall (www.aemet.es). Therefore, direct water uptake by the foliage may
477 positively contribute to water economy of holm oak during the summer. Since the
478 beginning of a storm (high or low precipitation), the environmental conditions (air
479 temperature and humidity, and vapour pressure deficit (VPD) sharply change as shown
480 in Figure 7 (data gathered with a Hobo Pro temp/RH (Onset Computer Bourne, MA,
481 USA) and a Rain Collector II (Davis Instruments, CA, USA)). The extreme VPD
482 reduction (close to 0 kPa, as simulated in our rehydration trials) provides optimal
483 conditions for foliar water absorption, since the low VPD retards the evaporation of
484 water drops hence increasing the chance for water uptake by the foliage.

485 An additional important source for leaf water absorption for evergreen holm oak is
486 the formation of dew due to condensation, which may occur all year round but may be
487 especially relevant during the summer. This mechanism occurs on approximately 20%
488 of summer days in the holm oak growing areas of the Iberian Peninsula
489 (www.aemet.es). Of the surface condensation mechanisms described (Nourbakhsh,

490 1989) two can be expected to occur under field conditions: (i) film condensation on the
491 wettable adaxial leaf side, and (ii) dropwise condensation on the unwettable abaxial
492 surface. While film condensation may lead to direct foliar water uptake, dropwise
493 condensation will favour drop dripping either to the soil or to the foliage below, which
494 may again turn available for foliar absorption. Finally, a further water deposition
495 phenomenon of limited relevance under Mediterranean conditions is the occurrence of
496 fog, in which the expected leaf wetting and water absorption mechanisms will be
497 similar to those described above for dew deposition.

498 It could be reckoned that adaxial leaf trichomes and scars may also contribute to
499 water loss and leaf dehydration. However, the mechanisms of uptake of liquid water and
500 loss probably as water vapour (Rockwell et al., 2014), and processes of water
501 adsorption and desorption in the cuticle (Reina et al., 2001) may be different and will
502 require further investigation. The functional advantage of water absorption by the upper
503 leaf side is not linked to a higher cuticular conductance, since no statistical differences
504 between adaxial and abaxial cuticular conductances were found.

505 In summary, in this study we analysed the water-leaf surface interactions of the
506 adaxial and abaxial leaf side of holm oak, a typical evergreen Mediterranean species.
507 While the adaxial trichomes present in young leaves were hydrophilic, the dense
508 indumentum of the lower leaf side led to a high degree of hydrophobicity. The upper
509 holm oak leaf side of young and mature leaves were wettable and absorbed water, and
510 the uptake mechanisms have been related to the presence of trichomes and trichomes
511 scars. It is concluded that trichome structure, chemical composition and function may
512 vary even for the same organ, but in relation to their occurrence in the abaxial versus the
513 adaxial leaf side. The water absorption capacity of holm oak leaves may be ecologically
514 advantageous for competition under Mediterranean conditions and in relation to
515 different means of water precipitation (e.g., condensation, rain or fog) all year round,
516 especially during summer and when growing in soils with low water storage capacity.

517

518

519 **MATERIALS AND METHODS**

520 **Plant material**

521 *Quercus ilex* L. seeds were planted in 500 ml containers filled with a mixture of 80%
522 substratum and 20% perlite and were kept in a greenhouse. Seedlings were transplanted
523 to 25 L containers after the first growing season, and they were subsequently
524 transplanted to an experimental field plot (CITA, Zaragoza, Spain). Plants always grew
525 under typically Mediterranean environmental conditions and were irrigated when
526 necessary, avoiding also the incidence of pests and diseases. Ten-year-old trees were
527 finally selected for the development of this study. Shoots with undamaged, fully
528 developed, 2-month old leaves with pubescent adaxial and abaxial sides (hereinafter
529 referred to as young leaves) were collected at early summer, whereas shoots having 8-
530 month old leaves (hereinafter referred to as mature leaves) with a glabrous adaxial and a
531 pubescent abaxial surface were collected at late autumn.

532 **Leaf surface water absorption**

533 By mid-June, two holm oak twigs per tree from five different trees of *Q. ilex* were
534 cut and enclosed in plastic bags until measurement. The initial water potential (Ψ_o) and
535 initial fresh weight (FW_o) were measured in three young shoots of each of the ten twigs
536 selected. Then, 2 mL of distilled water were carefully deposited on to: (i) the adaxial
537 side of the leaves of one of the shoots, and (ii) the abaxial side of the leaves of another
538 shoot. For comparison, the third shoot was used as an untreated control shoot.
539 Thereafter, young shoots were enclosed in single plastic bags and stored in the dark at
540 room temperature (at approximately 20° C). After 24 h, the weight and water potential
541 were measured again in all shoots to obtain the final water potential (Ψ_f) and final fresh
542 weight (FW_f). Then, shoots were dried in an oven (65°C, 24h) and they were weighed to
543 obtain the dry weight (DW). With the remaining young shoots of each twig not used in
544 this process, we obtained a relationship between shoot full saturation weight (turgid
545 weight, TW) and dry weight (DW). Afterwards, weight measurements were used to
546 calculate the relative water content (RWC) for each shoot as $RWC = (FW-DW)/(TW-$
547 $DW)$. A t-test paired sample comparison was used to compare leaf water potential and
548 relative water content before (Ψ_o , RWC_o) and after (Ψ_f , RWC_f) surface wetting. This
549 leaf surface water absorption process was repeated again at late autumn on mature
550 leaves.

551 **Cuticular conductance**

552 Cuticular water losses were measured gravimetrically on fully rehydrated young and
553 mature leaves (Anfodillo et al., 2002). To differentially assess the transpiration loss of
554 adaxial and abaxial surfaces, silicon grease was applied on to the opposite surface to
555 seal it against water loss. After initially weighing the leaves, they were placed for 72 h
556 in a dark chamber with an electric fan ensuring air circulation, under constant humidity
557 and temperature conditions (22.4 ± 0.1 °C and 76.4 ± 0.1 %). Cuticular conductance
558 (ms^{-1}) was calculated from the transpiration data and according to Anfodillo et al.
559 (2002).

560 **Quantitative and qualitative estimation of chemical components of holm oak**
561 **trichomes**

562 Adaxial and abaxial trichomes of young holm oak leaves were mechanically isolated
563 by gently scraping the leaf surfaces with a scalpel. Trichomes were subjected to the
564 successive removal of soluble cuticular lipids and cutin, while performing simultaneous
565 Fourier transformed infrared spectra (FTIR) analyses using a Nexus 670-870 NICOLET
566 FTIR spectrometer (Thermo Fisher Scientific, Waltham, USA; transmission mode, 3850
567 to 850 cm^{-1} with 4 cm^{-1} resolution, and accumulating 64 scans). For FTIR, samples were
568 ground with 1% potassium bromide, and thin tablets were subsequently formed and set
569 into the apparatus. A blank corresponding to the spectrum of potassium bromide was
570 also recorded and subtracted from sample spectra. For chemical removal, hairs were
571 first immersed in chloroform for 4 h, and then cutin was depolymerized by
572 saponification in 1M sodium hydroxide (KOH) for 24 h under reflux conditions.
573 Percentages of each chemical fraction (soluble waxes, cutin and remaining residue)
574 were calculated according to the corresponding weight loss.

575 Additionally, young holm oak leaves were enzymatically digested for four and seven
576 days in either 2% cellulase or 2% pectinase (both from Novozymes, Bagsvared,
577 Denmark) plus 2 mM sodium azide, adjusting the pH to 5.0 by adding sodium citrate.

578 **Microscopy**

579 Gold-sputtered intact and enzymatically digested adaxial and abaxial holm oak leaf
580 surfaces were examined with a variable pressure scanning electron microscope (SEM;
581 Hitachi S-3400 N, Tokyo, Japan; acceleration potential, 20 kV; working distance, 15-17

582 mm). Changes in adaxial and abaxial isolated trichome structure were analysed in intact
583 hairs, and after soluble lipid extraction and alkaline hydrolysis.

584 For transmission electron microscopy (TEM) Samples were fixed in 2.5%
585 glutaraldehyde-4% paraformaldehyde (both from Electron Microscopy Sciences (EMS),
586 Hatfield, USA) for 6 h at 4°C, rinsed in ice-cold phosphate buffer, pH 7.2, four times
587 within a period of 6 h and left overnight. Tissues were then post-fixed in a 1:1 2%
588 aqueous osmium tetroxide (TAAB Laboratories, Berkshire, UK) and 3% aqueous
589 potassium ferrocyanide (Sigma-Aldrich) solution for 1.5 h. Samples were then washed
590 with distilled water (x3), dehydrated in a graded series of 30, 50, 70, 80, 90, 95 and
591 100% acetone (x2, 15 min each concentration) and embedded in acetone-Spurr's resin
592 (TAAB Laboratories) solutions (3:1, 2h; 1:1; 2h; 1:3; 3h (v:v)) and in pure resin
593 overnight at room temperature. Final embedding was done in blocks which were
594 incubated at 70°C for 3 days for complete polymerization. Prior to TEM observation,
595 sections were post-stained with Reynolds lead citrate (EMS) for 5 min.

596 Thin, cryo-sectioned leaf tissues (30 μ thick) were observed with a Olympus BX40
597 fluorescence microscope. Transversal sections were examined by either visible light
598 transmission or under UV excitation (emission of blue fluorescence by simple phenols
599 and lignin) after immersion in 10% (w:v) KOH for 2 min, followed by a thorough
600 distilled water rinse. A U-MWU filter combination (exciter filter 330-385 nm, barrier
601 filter 420 nm) was used. Leaf sections were also stained with Sudan IV.
602 Microphotographs were taken using a Olympus DP71 digital camera (Olympus
603 Corporation, Tokyo, Japan).

604 The average number of trichome arms, arm length, arm diameter, trichome densities,
605 and leaf area covered with hairs were assessed by image analysis of adaxial and abaxial
606 SEM micrographs (ImageJ 1.45s, W.R., National Institutes of Health, Bethesda,
607 Maryland, USA).

608 **Contact angle determinations and leaf surface properties**

609 Advancing contact angles (θ) of drops of double-distilled water, glycerol and
610 diiodomethane (both 99% purity; Sigma-Aldrich) were measured at room temperature
611 (25°C) using a CAM 200 contact angle meter (KSV Instruments, Helsinki, Finland)
612 equipped with a CCD camera, frame grabber and image analysis software. Contact
613 angles were determined on adaxial and abaxial surfaces of intact, young and mature
614 leaves. After removing the midrib and margins, leaf sections of approximately 2 x 0.5

615 cm² were cut with a scalpel and mounted on a microscope slide with double-sided
616 adhesive tape. Two μ L drops of each liquid were deposited onto the adaxial or abaxial
617 holm leaf surfaces with a manual dosing system holding a 1 mL syringe with 0.5 mm
618 diameter needle (30 repetitions). Side view images of the drops were captured at a rate
619 of 6 frames s⁻¹. Contact angles were automatically calculated by fitting the captured
620 drop shape to the one calculated from the Young-Laplace equation. For mature leaves
621 and all abaxial leaf surfaces, θ for all the liquids were measured shortly after drop
622 deposition. On young adaxial surfaces, however, the θ of water and chiefly glycerol
623 were initially high and decreased over time. Hence, θ values were recorded immediately
624 after drop deposition and also when they were static (taking approximately 15 sec for
625 water and 10 min for glycerol).

626 For all the surfaces evaluated, the total surface free energy or surface tension (γ) and
627 its components, i.e. the Lifshitz-van der Waals (γ^{LW}) and acid-base (γ^{AB} ; γ^+ and γ^-)
628 components, as well as the work-of-adhesion for the three liquids and the solubility
629 parameter were calculated, considering the surface tension components of water ($\gamma^{LW} =$
630 21.8 mJ m^{-2} , $\gamma^+ = \gamma^- = 25.5 \text{ mJ m}^{-2}$), glycerol ($\gamma^{LW} = 34.0 \text{ mJ m}^{-2}$, $\gamma^+ = 3.92 \text{ mJ m}^{-2}$, $\gamma^- =$
631 57.4 mJ m^{-2}) and diiodomethane ($\gamma^{LW} = 50.8 \text{ mJ m}^{-2}$, $\gamma^+ = \gamma^- = 0 \text{ mJ m}^{-2}$) (Fernández et
632 al., 2011; Khayet and Fernández, 2012).

633

634 LITERATURE CITED

- 635 **Adamec L** (2013) Foliar mineral nutrient uptake in carnivorous plants: what do we
636 know and what should we know? *Front Plant Sci* **4**: 10
- 637 **Allen RG, Walter IA, Elliott B, Mechan B, Jensen ME, Itentisu D, Howell TA,**
638 **Snyder R, Brown P, Eching S, Spofford, Hettendorf M, Cuenca RH, Wright JL,**
639 **Martin D** (2000) Issues, requirements and challenges in selecting and specifying and
640 standardized ET equation. Proc 4th National Irrig Symp ASAE, Phoenix, AZ, pp
641 201-204
- 642 **Anfodillo T, Pasqua di Bisceglie D, Urso T** (2002) Minimum cuticular conductance
643 and cuticle features of *Picea abies* and *Pinus cembra* needles along an altitudinal
644 gradient in the Dolomites (NE Italian Alps). *Tree Physiol* **22**: 479-487
- 645 **Aryal B, Neuner G** (2010) Leaf wettability decreases along an extreme altitudinal
646 gradient. *Oecologia* **162**: 1-9
- 647 **Benzing DH, Henderson K, Kessel B, Sulak J** (1976) The absorptive capacities of
648 bromeliad trichomes. *Am J Bot* **63**:1009-1014
- 649 **Berry ZC, Smith WK** (2012) Cloud pattern and water relations in *Picea rubens* and
650 *Abies fraseri* southern Appalachian Mountains, USA. *Agric Forest Meteorol* **162**:
651 27-34

- 652 **Berry ZC, Hughes NM, Smith WK** (2013) Cloud immersion: an important water
653 source for spruce and fir saplings in the southern Appalachian Mountains. *Oecologia*
654 **173** (3): 637-648
- 655 **Berry ZC, Hughes NM, Smith WK** (2014) Cloud immersion: an important water
656 source for spruce and fir saplings in the southern Appalachian Mountains. *Oecologia*
657 **174** (2), 319-326
- 658 **Breshears DD, McDowell NG, Goddard KL, Dayem KE, Martens SN, Meyer CW,**
659 **Brown KM** (2008) Foliar absorption of intercepted rainfall improves woody plant
660 water status most during drought. *Ecology* **89**: 41-47
- 661 **Brewer CA, Smith WK, Vogelmann TC** (1991) Functional interaction between leaf
662 trichomes, leaf wettability and the optical properties of water droplets. *Plant Cell*
663 *Environ* **14**: 955-962
- 664 **Brewer CA, Smith WK** (1997) Patterns of leaf surface wetness for montane and
665 subalpine plants. *Plant Cell Environ* **20**: 1-11
- 666 **Brewer CA, Nuñez CI** (2007) Patterns of leaf wettability along an extreme moisture
667 gradient in western Patagonia, Argentina. *Int J Plant Sci* **168**: 555-562
- 668 **Burgess SSO, Dawson TE** (2004) The contribution of fog to the water relations of
669 *Sequoia sempervirens* (D. Don): foliar uptake and prevention of dehydration. *Plant*
670 *Cell Environ* **27**: 1023-1034
- 671 **Burkhardt J, Basi S, Pariyar S, Hunsche M** (2012) Stomatal penetration by aqueous
672 solutions – an update involving leaf surface particles. *New Phytol* **196**: 774-787
- 673 **Burkhardt J, Hunsche M** (2013) “Breath figures” on leaf surfaces – formation and
674 effects of microscopic leaf wetness. *Front Plant Sci* **4**: 422
- 675 **Burrows GE, White RG, Harper JD, Heady RD, Stanton RA, Zhu X, Wu H,**
676 **Lemerle D** (2013) Intrusive trichome bases in the leaves of silverleaf nightshade
677 (*Solanum elaeagnifolium*; *Solanaceae*) do not facilitate fluorescent tracer uptake. *Am*
678 *J Bot* **100**: 2307-2317
- 679 **Camarero JJ, Olano JM, Arroyo Alfaro SJ, Fernández-Marín B, Becerril JM,**
680 **García-Plazaola JI** (2012) Photoprotection mechanisms in *Quercus ilex* under
681 contrasting climatic conditions. *Flora* **207**: 557-564
- 682 **Dietz J, Leuschner C, Hölscher D, Kreilein H** (2007) Vertical patterns and duration
683 of surface wetness in an old-growth tropical montane forest, Indonesia. *Flora* **202**:
684 111-111
- 685 **Domínguez E, Heredia-Guerrero JA, Heredia A** (2011) The biophysical design of
686 plant cuticles: an overview. *New Phytol* **189**: 938-949
- 687 **Ehleringer JR, Björkman O** (1978) A comparison of photosynthetic characteristics of
688 *Encelia* species possessing glabrous and pubescent leaves. *Plant Physiol* **62**: 185-190
- 689 **Eigenbrode SD, Jetter R** (2002). Attachment to plant surface waxes by an insect
690 predator. *Integr Comp Biol* **42**: 1091-1099
- 691 **Fahn A** (1986) Structural and functional properties of trichomes of xeromorphic leaves.
692 *Ann Bot* **57**: 631-637
- 693 **Fernández V, Eichert T** (2009) Uptake of hydrophilic solutes through plant leaves:
694 current state of knowledge and perspectives of foliar fertilization. *Crit Rev Plant Sci*
695 **28**: 36-68
- 696 **Fernández V, Khayet M, Montero-Prado P, Heredia-Guerrero JA, Liakoulouos G,**
697 **Karabourniotis G, Del Río V, Domínguez E, Tacchini I, Nerín C, Val J, Heredia**
698 **A** (2011) New insights into the properties of pubescent surfaces: peach fruit as
699 model. *Plant Physiol* **156**: 2098-2108
- 700 **Fernández V, Brown PH** (2013) From plant surface to plant metabolism: the uncertain
701 fate of foliar-applied nutrients. *Front Plant Sci* **4**: 289

- 702 **Fernández V, Guzmán P, Peirce CAE, McBeath TM, Khayet M, McLaughlin MJ**
703 (2014) Effect of wheat phosphorus status on leaf surface properties and permeability
704 to foliar applied phosphorus. *Plant Soil*: in press, doi: 10.1007/s11104-014-2052-6
- 705 **Gniwotta F, Vogg G, Gartmann V, Carver TL, Riederer M, Jetter R** (2005) What
706 do microbes encounter at the plant surface? Chemical composition of pea leaf
707 cuticular waxes. *Plant Physiol* **139**: 519-530
- 708 **Gotsch SG, Asbjornsen H, Holwerda F, Goldsmith GR, Weintraub AE, Dawson**
709 **TE** (2014) Foggy days and dry nights determine crown-level water balance in a
710 seasonal tropical Montane cloud forest. *Plant Cell Environ* **37**:261-72
- 711 **Grammatikopoulos G, Manetas Y** (1994) Direct absorption of water by hairy leaves
712 of *Phlomis fruticosa* and its contribution to drought avoidance. *Can J Bot* **72**: 1805-
713 1811
- 714 **Guzmán P, Fernández V, Khayet M, Gil ML, Fernández A, Gil L** (2014a)
715 Ultrastructure of plant leaf cuticles in relation to sample preparation as observed by
716 transmission electron microscopy. *Sci World J*, Article ID **963921**, 9 pp
- 717 **Guzmán P, Fernández V, García ML, Khayet M, Fernández A, Gil L** (2014b)
718 Localization of polysaccharides in isolated and intact cuticles of eucalypt, poplar and
719 pear leaves by enzyme-gold labeling. *Plant Physiol Biochem* **76**: 1-6
- 720 **Hanba YT, Moriya A, Kimura K** (2004) Effect of leaf surface wetness and wettability
721 on photosynthesis in bean and pea. *Plant Cell Environ* **27**: 413-421
- 722 **Hardin JW** (1976) Terminology and classification of *Quercus* trichomes. *J Elisha*
723 *Mitch Sci S* **92**: 151-161
- 724 **Helliker BR, Griffiths H** (2007) Towards a plant-based proxy for the isotope ratio of
725 atmospheric water vapor. *Globl Change Biol* **13**:723-733
- 726 **Helliker BR** (2014) Reconstructing the $\delta^{18}\text{O}$ of atmospheric water vapour via the CAM
727 epiphyte *Tillandsia usneoides*: seasonal controls on $\delta^{18}\text{O}$ in the field and large-scale
728 reconstruction of $\delta^{18}\text{O}_a$. *Plant Cell Environ* **37**: 541-556
- 729 **Holder CD** (2007a) Leaf water repellency of species in Guatemala and Colorado (USA)
730 and its significance to forest hydrology studies. *J Hydrol* **336**: 147-154
- 731 **Holder CD** (2007b) Leaf water repellency as an adaptation to tropical montane cloud
732 forest environments. *Biotropica* **39**: 767-770
- 733 **Javelle M, Vernoud V, Rogowsky PM, Ingram GC** (2011) Epidermis: the formation
734 and functions of a fundamental plant tissue. *New Phytol* **189**: 17-39
- 735 **Johnson HB** (1975) Plant pubescence: an ecological perspective. *Bot Rev* **41**: 233-258
- 736 **Johnstone JA, Dawson TE** (2010) Climatic context and ecological implications of
737 summer fog decline in the coast redwood region. *P Natl Acad Sci USA* **107**: 4533-
738 4538
- 739 **Karabourniotis G, Papadopoulos K, Papamarkou M, Manetas Y** (1992) Ultraviolet-
740 B radiation absorbing capacity of leaf hairs. *Physiol Plantarum* **86**: 414-418
- 741 **Karabourniotis G, Kotsabassidis D, Manetas Y** (1995) Trichome density and its
742 protective potential against ultraviolet-B radiation damage during leaf development.
743 *Can J Bot* **73**: 376-383
- 744 **Karabourniotis G, Kofidis G, Fasseas C, Liakoura V, Drossopoulos I** (1998)
745 Polyphenol deposition in leaf hairs of *Olea europaea* (*Oleaceae*) and *Quercus ilex*
746 (*Fagaceae*). *Am J Bot* **85**: 1007-1012
- 747 **Karabourniotis G, Bormann JF** (1999) Penetration of UV-A UV-B and blue light
748 through the leaf trichome of two xeromorphic plants, olive and oak, measured by
749 optical fibre microprobes. *Physiol Plantarum* **105**: 655-661
- 750 **Karioti A, Sokovic M, Ciric A, Koukoulitsa C, Bilia AR, Skaltsa H** (2011)
751 Antimicrobial properties of *Quercus ilex* L. proanthocyanidin dimers and simple

- 752 phenolics: evaluation of their synergistic activity with conventional antimicrobials
753 and prediction of their pharmacokinetic profile. *J Agr Food Chem* **59**: 6412-6422
- 754 **Kenzo T, Yoneda R, Azani MA, Majid NM** (2008) Changes in leaf water use after
755 removal of leaf lower surface hairs on *Mallotus macrostachyus* (*Euphorbiaceae*) in a
756 tropical secondary forest in Malaysia. *J Forest Res* **13**: 137-142
- 757 **Khayet M, Fernández V** (2012) Estimation of the solubility parameter of model plant
758 surfaces and agrochemicals: a valuable tool for understanding plant surface
759 interactions *Theor Biol Med Mod* **9**: 45
- 760 **Kim K Lee X** (2011) Transition of stable isotope ratios of leaf water under simulated
761 dew formation. *Plant Cell Environ* **34**: 1790-1801
- 762 **Koch K, Barthlott W** (2009) Superhydrophobic and super- hydrophilic plant surfaces:
763 an inspiration for biomimetic materials. *Philos T R Soc A* **367**: 1487-1509
- 764 **Konrad W, Ebner M, Traiser C, Roth-Nebelsick A** (2012) Leaf surface wettability
765 and implications for drop shedding and evaporation from forest canopies. *Pure Appl*
766 *Geophys* **169**: 835-845
- 767 **Kwok DY, Neumann AW** (1999) Contact angle measurement and contact angle
768 interpretation. *Adv Colloid Interfac* **81**: 167-249
- 769 **Łaźniewska J, Macioszek VK, Kononowicz AK** (2012) Plant-fungus interface: The
770 role of surface structures in plant resistance and susceptibility to pathogenic fungi.
771 *Physiol Mol Plant P* **78**: 24-30
- 772 **Liakopoulos G, Nikolopoulos D, Klouvatou A, Vekkos KA, Manetas Y,**
773 **Karabourniotis G** (2006) The photoprotective role of epidermal anthocyanins and
774 surface pubescence in young leaves of grapevine (*Vitis vinifera* L.). *Ann Bot* **98**:
775 257-265
- 776 **Limm EB, Simonin KS, Bothman AG, Dawson TE** (2009) Foliar water uptake: A
777 common water acquisition strategy for plants of the redwood forest. *Oecologia* **161**:
778 449-459
- 779 **Limm EB, Dawson TE** (2010) *Polystichum munitum* (*Dryopteridaceae*) varies
780 geographically in its capacity to absorb fog water by foliar uptake within the
781 redwood forest ecosystem. *Am J Bot* **97**: 1121-1128
- 782 **Martin CE, von Willert DJ** (2000) Leaf epidermal hydathodes and the
783 ecophysiological consequences of foliar water uptake in species of *Crassula* from the
784 Namib desert in Southern Africa. *Plant Biol* **2**: 229-242
- 785 **Martins CMC, Mesquita SMM, Vaz WLC** (1999) Cuticular waxes of the holm
786 (*Quercus ilex* L. subsp. *ballota* (Desf.) Samp.) and cork (*Q. suber* L.) oaks.
787 *Phytochem Analysis* **10**: 1-5
- 788 **Morales F, Abadía A, Abadía J, Montserrat G, Gil-Pelegrín E** (2002) Trichomes
789 and photosynthetic pigment composition changes: responses of *Quercus ilex* subsp.
790 *ballota* (Desf.) Samp. and *Quercus coccifera* L. to Mediterranean stress conditions.
791 *Trees* **16**: 504-510
- 792 **Mosmann V, Castro A, Fraile R, Dessens J, Sanchez JL** (2004) Detection of
793 statistically significant trends in the summer precipitation of mainland Spain. *Atmos*
794 *Res* **70**: 43-53
- 795 **Nikolopoulos D, Liakopoulos G, Drossopoulos I, Karabourniotis G** (2002) The
796 relationship between anatomy and photosynthetic performance of heterobaric leaves.
797 *Plant Physiol* **129**: 235-243
- 798 **Nourbakhsh HP** (1989) Two-phase heat transfer. In EC Guyer, ed, *Handbook of*
799 *Applied Thermal Design*. McGraw-Hill, New York, pp 75-84

- 800 **Oliveira RS, Dawson TE, Burgess SO** (2005) Evidence for direct water absorption by
801 the shoot of the desiccation-tolerant plant *Vellozia flavicans* in the savannas of
802 central Brazil. *J Tropical Ecol* **21**: 585-588
- 803 **Pandey S, Nagar PK** (2003) Pattern of leaf surface wetness in some important
804 medicinal and aromatic plants of western Himalaya. *Flora* **198**: 349-357
- 805 **Pierce S, Maxwell K, Griffiths H, Winter K** (2001) Hydrophobic trichome layers and
806 epicuticular wax powders in *Bromeliaceae*. *Am J Bot* **88**: 1371-1389
- 807 **Ramírez FJ, Luque P, Heredia A, Bukovac MJ** (1992) Fourier transform IR study of
808 enzymatically isolated tomato fruit cuticular membrane. *Biopolymers* **32**:1425-1429
- 809 **Reicosky DA, Hanover JW** (1978) Physiological effects of surface waxes. *Plant*
810 *Physiol* **62**: 101-104
- 811 **Reina JJ, Domínguez E, Heredia A** (2001) Water sorption–desorption in conifer
812 cuticles: The role of lignin. *Physiol Plantarum* **112**: 372-378
- 813 **Reyes-García C, Mejia-Chang M, Griffiths H** (2012) High but not dry: diverse
814 epiphytic bromeliad adaptations to exposure within a seasonally dry tropical forest
815 community. *New Phytol* **193**: 745-754
- 816 **Riederer M, Schreiber L** (2001) Protecting against water loss: analysis of the barrier
817 properties of plant cuticles. *J Exp Bot* **52**: 2023-2032
- 818 **Riederer M** (2006). Introduction: biology of the plant cuticle. In M Riederer, C Müller
819 C, eds, *Biology of the plant cuticle*, Annual Plant Reviews Vol 23. Blackwell
820 Publishing, Oxford, pp 1-10
- 821 **Ripley BS, Pammenter NW, Smith VR** (1999) Function of leaf hairs revisited: The
822 hair layer on leaves *Arctotheca populifolia* reduces photoinhibition, but leads to
823 higher leaf temperatures caused by lower transpiration rates. *J Plant Physiol* **155**: 78-
824 85
- 825 **Rockwell FE, Holbrook NM, Stroock AD** (2014) The competition between liquid and
826 vapor transport in transpiring leaves. *Plant Physiol* **164**: 1741-1758
- 827 **Rosado BHP, Holder CD** (2013) The significance of leaf water repellency in
828 ecohydrological research: a review. *Ecohydrol* **6**: 150-161
- 829 **Roth-Nebelsick A, Hassiotou F, Veneklaas EJ** (2009) Stomatal crypts have small
830 effects on transpiration: a numerical model analysis. *Plant Physiol* **151**: 2018-2027
- 831 **Roth-Nebelsick A, Ebner M, Miranda T, Gottschalk V, Voigt D, Gorb S,**
832 **Stegmaier T, Sarsour J, Linke M, Konrad W** (2012) Leaf surface structures
833 enable the endemic Namib desert grass *Stipagrostis sabulicola* to irrigate itself with
834 fog water. *J R Soc Interface* **9**: 1965-1974
- 835 **Schlegel TK, Schönherr J** (2002) Stage of development affects penetration of calcium
836 chloride into apple fruits. *J Plant Nutr Soil Sc* **165**:738-745
- 837 **Schönherr J, Bukovac MJ** (1972) Penetration of stomata by liquids. Dependence on
838 surface tension, wettability, and stomatal morphology. *Plant Physiol* **49**: 813-819
- 839 **Simonin KA, Santiago LS, Dawson TE** (2009) Fog interception by *Sequoia*
840 *sempervirens* (D. Don) crowns decouples physiology from soil water deficit. *Plant*
841 *Cell Environ* **32**: 882-892
- 842 **Urrego-Pereira YF, Martínez-Cob A, Fernández V, Caverro J** (2013) Daytime
843 sprinkler irrigation effects on net photosynthesis of maize and alfalfa. *Agron J* **105**:
844 1515-1528
- 845 **van Oss CJ, Chaudhury MK, Good RJ** (1987) Monopolar surfaces. *Adv Colloid*
846 *Interface Sci* **28**: 35-64
- 847 **van Oss CJ, Chaudhury MK, Good RJ** (1988) Interfacial Lifshitz-van der Waals and
848 polar interactions in macroscopic systems. *Chem Rev* **88**: 927-941

- 849 **Villena JF, Domínguez E, Heredia A** (2000) Monitoring biopolymers present in plant
850 cuticles by FT-IR spectroscopy. *J Plant Physiol* **156**: 419-422
- 851 **Yates DJ, Hutley LB** (1995) Foliar uptake of water by wet leaves of *Sloanea woollsii*,
852 an Australian subtropical rainforest tree. *Aust J Bot* **43**: 157-167
- 853 **Yeats TH, Rose JK** (2013) The formation and function of plant cuticles. *Plant Physiol*
854 **163**: 5-20
- 855 **Wagner GJ, Wang E, Shepherd RW** (2004) New approaches for studying and
856 exploiting an old protuberance, the plant trichome. *Ann Bot* **93**: 3-11
- 857 **Wen XF, Lee X, Sun XM, Wang JL, Hu ZM, Li SG, Yu GR** (2012) Dew water
858 isotopic ratios and their relationships to ecosystem water pools and fluxes in a
859 cropland and a grassland in China. *Oecologia* **168**: 549-561
- 860 **Werker E** (2000) Trichome diversity and development. *Adv Bot Res* **31**: 1-35
- 861 **Wylie RB** (1943) The role of the epidermis in foliar organization and its relations to the
862 minor venation. *Am J Bot*: 273-280
- 863

864 **TABLES**

865

Table I. *Contact angles of water (θ_w), glycerol (θ_g) and diiodomethane (θ_d) with the adaxial and abaxial surface of young and mature holm oak leaves*

Leaf age	θ_w (°)		θ_g (°)		θ_d (°)	
	Adaxial	Abaxial	Adaxial	Abaxial	Adaxial	Abaxial
Young	40.7±3.8	130.1±6.5	50.2±5.1	141.4±4.4	56.6±4.9	128.4±6.5
	91.1±6.0 ⁱ		143.5±6.0 ⁱ			
Mature	55.5±5.1	134.3±10.1	68.6±5.9	142.5±3.9	59.1±4.1	119.3±10.2

866 ⁱInitial θ of H₂O and glycerol when deposited on to the adaxial young leaf surfaces.867 The remaining θ values were recorded when the drops were stable and did not vary

868 when deposited on to the surfaces.

869

Table II. Surface free energy per unit of area. Lifshitz van der Waals component (γ^{LW}), Acid-base component (γ^{AB}), total surface free energy (γ) and surface polarity ($\gamma^{AB} \gamma^{-1}$) of the adaxial and abaxial surface of young and mature holm oak leaves

Leaf side	γ^{LW} (mJ m ⁻²)		γ^{AB} (mJ m ⁻²)		γ (mJ m ⁻²)		$\gamma^{AB} \gamma^{-1}$ (%)	
	Young	Mature	Young	Mature	Young	Mature	Young	Mature
Adaxial	30.55	29.11	12.50	0.55	43.05	29.66	29.04	1.85
Abaxial	1.82	3.31	2.42	2.45	4.24	5.76	57.02	42.53

871

872

873

Table III. Solubility parameter (δ) and work-of-adhesion for water ($W_{a,w}$), glycerol ($W_{a,g}$) and diiodomethane ($W_{a,d}$) and solubility parameter (δ) of intact, adaxial and abaxial surfaces of young and mature holm oak leaves

Leaf age	$W_{a,w}$ (mJ m ⁻²)		$W_{a,g}$ (mJ m ⁻²)		$W_{a,d}$ (mJ m ⁻²)		δ (MJ ^{1/2} m ^{-3/2})	
	Adaxial	Abaxial	Adaxial	Abaxial	Adaxial	Abaxial	Adaxial	Abaxial
Young	127.99	25.93	104.98	14.00	78.79	19.25	20.85	3.67
Mature	114.04	21.99	87.40	13.25	76.91	25.94	15.77	4.62

875

876

877 **FIGURES LEGENDS**

878

879 **Figure 1. Leaf water potential (ψ) and relative water content (RWC) for young (A,**
880 **C) and mature (B, D) shoots of *Q. ilex* before (grey bars) and after (black bars)**
881 **surface wetting.** AdW = leaf adaxial wetting; AbW = leaf abaxial wetting; NW = no
882 wetting. Significant difference before and after surface wetting were found in all cases.

883

884 **Figure 2. SEM micrographs of intact adaxial and abaxial holm oak leaf surfaces.**
885 (A, B) Adaxial and abaxial sides of young leaves, (C, D) adaxial and abaxial sides of
886 mature leaves.

887

888 **Figure 3. Optical and transmission electron microscopy micrographs of intact**
889 **adaxial and abaxial surfaces of holm oak young (A to F) and mature (G) leaves.**
890 (A) transversal section of a young leaf stained with Sudan IV, (B) adaxial leaf trichome,
891 (C) abaxial leaf trichome, (D) base of an adaxial leaf trichome observed by TEM, (E)
892 base of an abaxial leaf trichome observed by TEM, (F) detail of scar on a young, adaxial
893 leaf surface after trichome shedding, and (G) detail of two scars on a mature, adaxial
894 leaf surface after trichome shedding. Note that the bases are near the bundle sheath extension
895 (dark blue).

896

897 **Figure 4. FTIR spectra of isolated (A), dewaxed (B), and cutin depolymerized (C)**
898 **abaxial holm oak leaf trichomes.**

899

900

901 **Figure 5. Isolated trichomes of adaxial and abaxial holm oak leaf surfaces after**
902 **gradual extraction of chemical components.** (A, B) intact trichomes, (C, D) trichomes
903 after chloroform extraction, and (E, F) trichomes after cutin depolymerization.

904

905 **Figure 6. Effect of cellulose hydrolysis on holm oak adaxial (A, B, C) and abaxial**
906 **(D) leaf surfaces.** (A) intact, adaxial leaf surface, (B) adaxial leaf surface after 4 days in
907 cellulase solution, (C) adaxial leaf surface after 7 days in cellulase solution, and (D)
908 abaxial leaf surface after 7 days in cellulase solution.

909

910 **Figure 7. Hourly evolution of Temperature (T), Relative Humidity (RH) and**
911 **Vapor Pressure Deficit (VPD) during five consecutive summer days in a typically**
912 **Mediterranean holm oak area.** The gray area indicates a precipitation event lower
913 than 1 mm.

Young shoots

Mature shoots

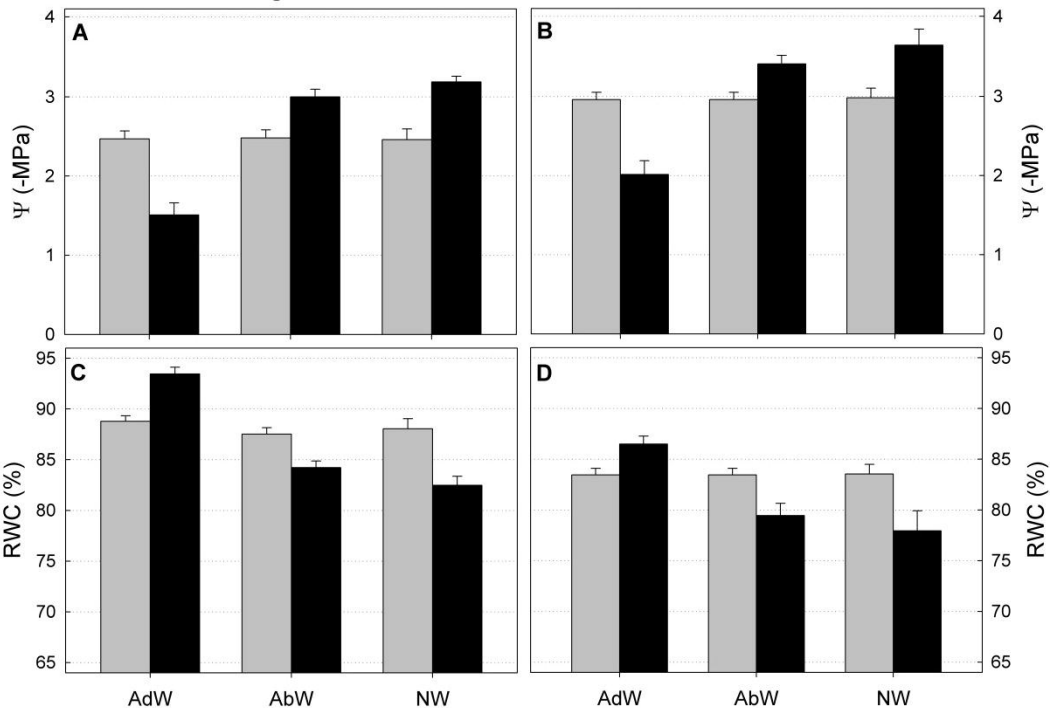


Figure 1. Leaf water potential (ψ) and relative water content (RWC) for young (A, C) and mature (B, D) shoots of *Q. ilex* before (grey bars) and after (black bars) surface wetting. AdW = leaf adaxial wetting; AbW = leaf abaxial wetting; NW = no wetting. Significant differences before and after surface wetting were found in all cases.

Downloaded from www.plantphysiol.org on June 20, 2014 - Published by American Society of Plant Biologists. All rights reserved. Copyright © 2014 American Society of Plant Biologists.

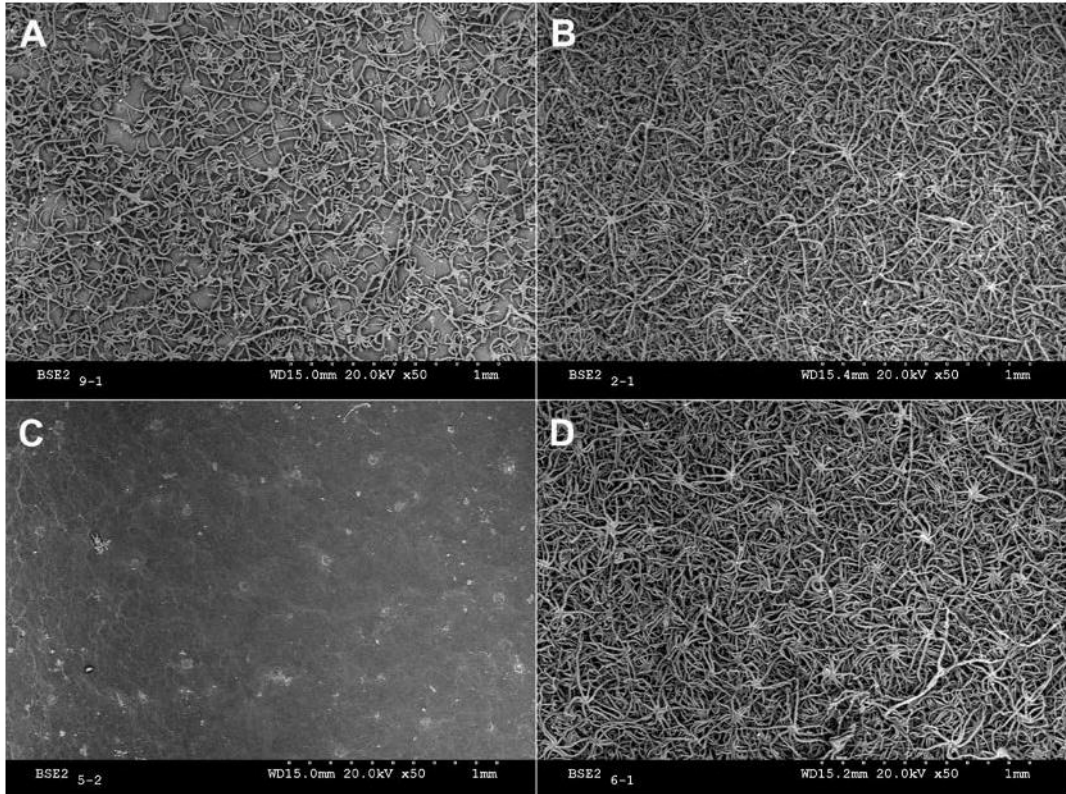


Figure 2. SEM micrographs of intact adaxial and abaxial holm oak leaf surfaces. (A, B) Adaxial and abaxial sides of young leaves, (C, D) adaxial and abaxial sides of mature leaves.

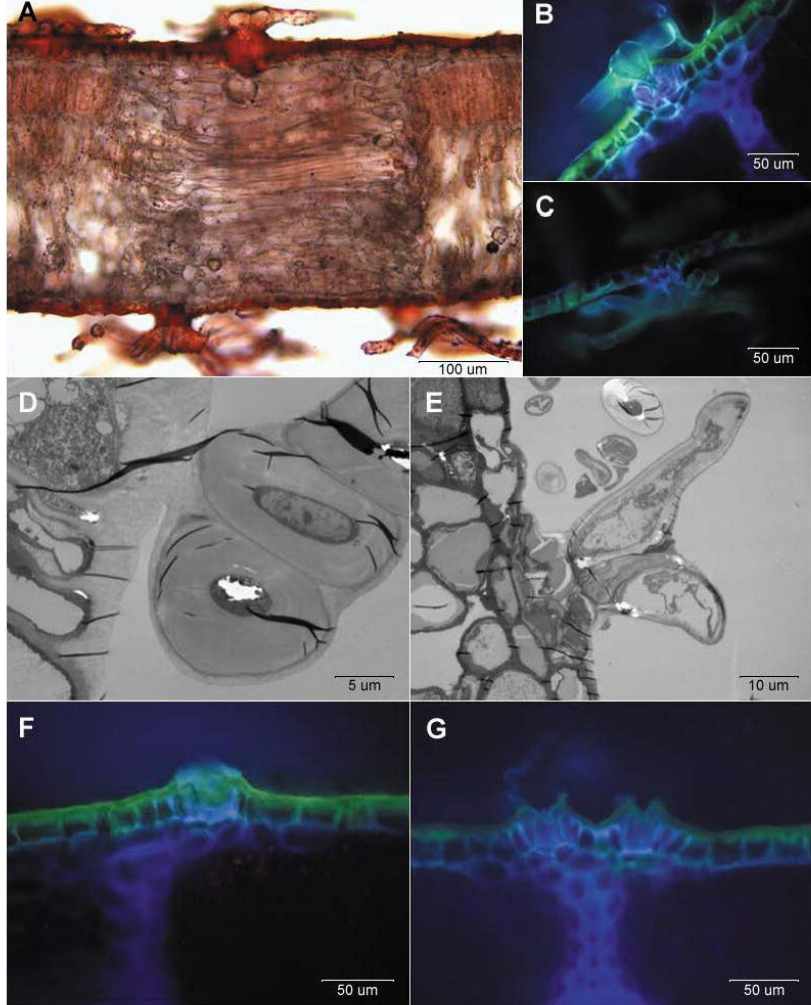


Figure 3. Optical and transmission electron microscopy micrographs of intact adaxial and abaxial surfaces of holm oak young (A to F) and mature (G) leaves. (A) transversal section of a young leaf stained with Sudan IV, (B) adaxial leaf trichome, (C) abaxial leaf trichome, (D) base of an adaxial leaf trichome observed by TEM, (E) base of an abaxial leaf trichome observed by TEM, (F) detail of scar on a young, adaxial leaf surface after trichome shedding, and (G) detail of two scars on a mature, adaxial leaf surface after trichome shedding. Note that the bases are near the bundle sheath extension (dark blue).

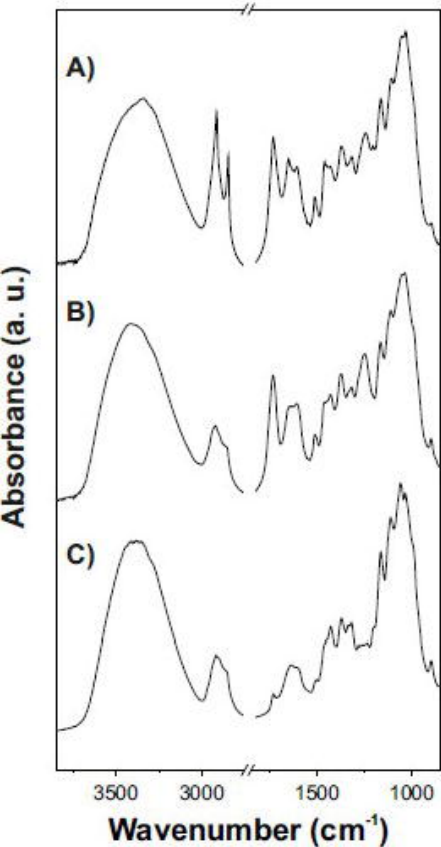


Figure 4. FTIR spectra of isolated (A), dewaxed (B), and cutin depolymerized (C) abaxial holm oak leaf trichomes.

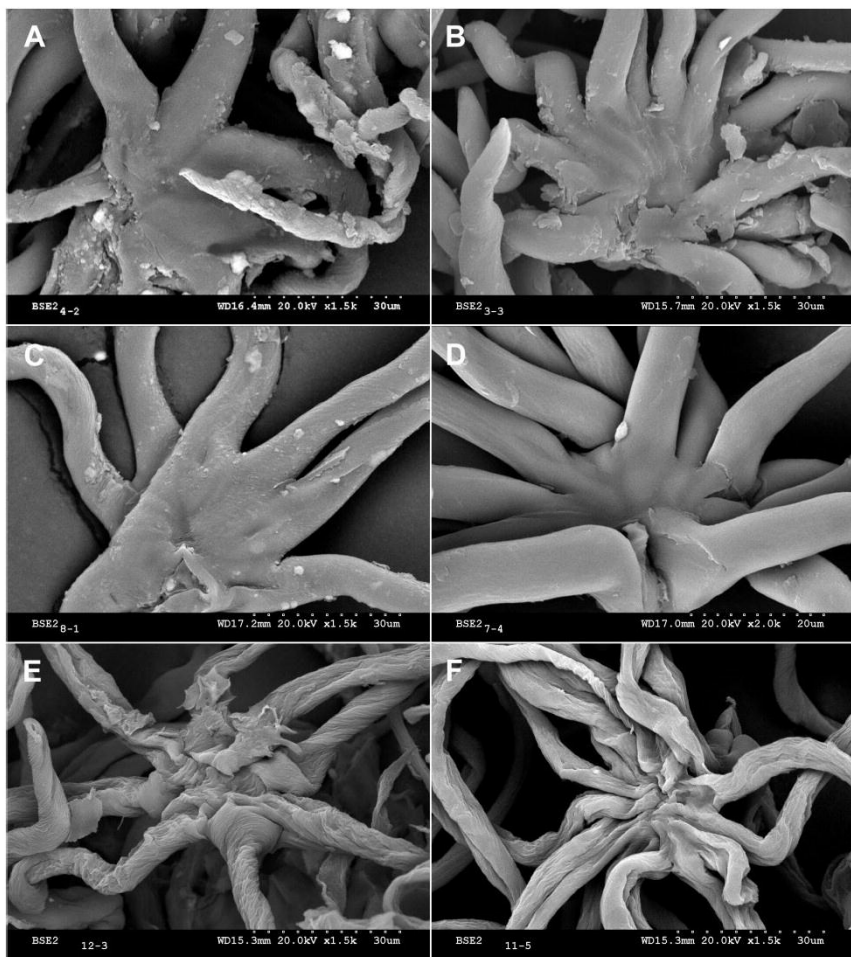


Figure 5. Isolated trichomes of adaxial and abaxial holm oak leaf surfaces after gradual extraction of chemical components. (A, B) intact trichomes, (C, D) trichomes after chloroform extraction, and (E, F) trichomes after depolymerization.



Figure 6. Effect of cellulose hydrolysis on holm oak adaxial (A, B, C) and abaxial (D) leaf surfaces. (A) intact, adaxial leaf surface, (B) adaxial leaf surface after 4 days in cellulase solution, (C) adaxial leaf surface after 7 days in cellulase solution, (D) abaxial leaf surface after 7 days in cellulase solution.

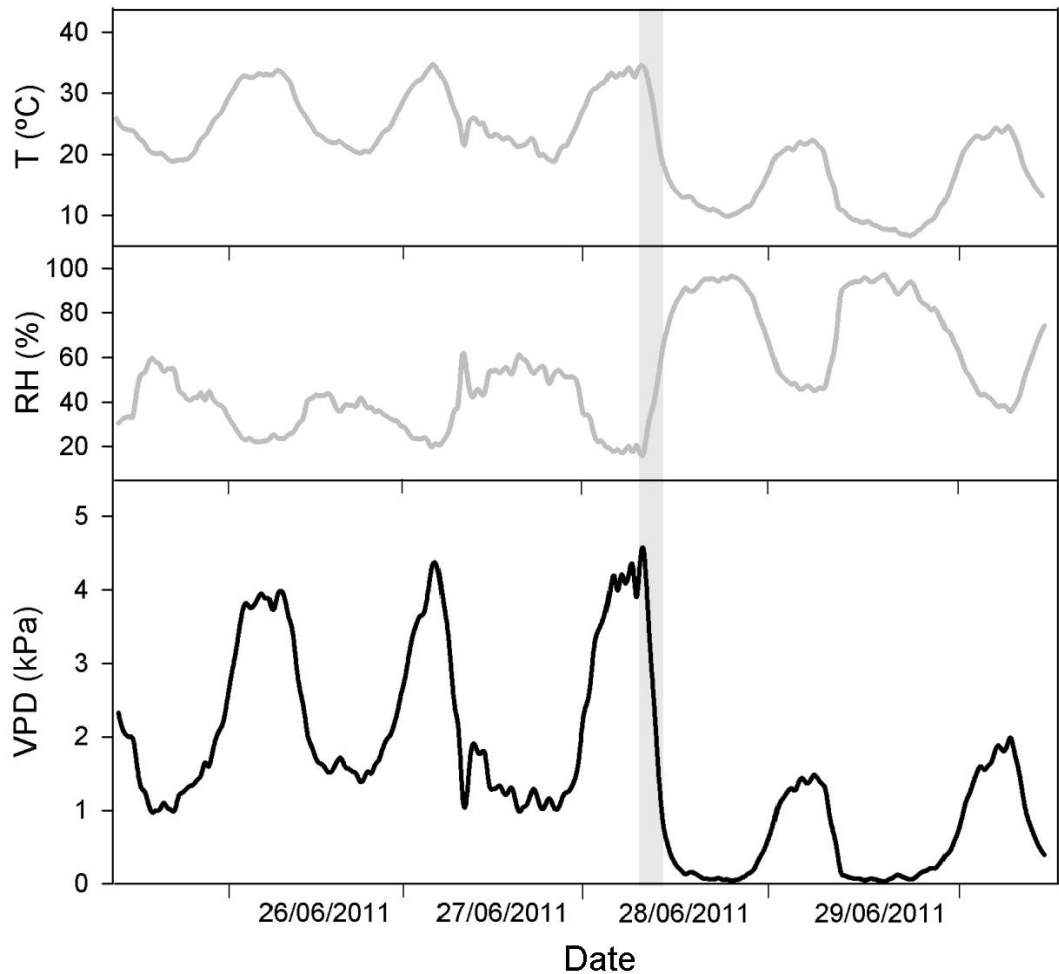


Figure 7. Hourly evolution of Temperature (T), Relative Humidity (RH) and Vapour Pressure Deficit (VPD) during five consecutive summer days in a typically Mediterranean holm oak area. Downloaded from www.plantphysiol.org on June 20, 2014 - Published by American Society of Plant Biologists. All rights reserved. Copyright © 2014 American Society of Plant Biologists. All rights reserved.

precipitation event lower than 1 mm.